Surface-Depended Growth Kinematics in Euclidean 3-space E^3

Sezen Öncül [1,*], Zehra Özdemir[2], İsmail Gök [3]

[1,3]Department of Mathematics, Faculty of Science, University of Ankara, 06100 Ankara, Turkey

[3]Department of Mathematics, Arts and Science Faculty, Amasya University, 05189 Amasya, Turkey

Abstract

In this paper, we investigate the surface-dependent growth model in Euclidean 3-space. The surface-dependent model is developed to model the kinematics of surface growth for objects that can be generated by the curves on the surface, such as parasites and plants. This paper includes two main purposes for this model. The first one is to parameterize this model by using the quaternions and homothetic motions. Furthermore, we express the matrix representations of the surface-dependent growth model. The second one is to construct the surface-dependent growth model by using the growth velocity components related to the Darboux frame at each point of the generating curve. Moreover, to support the theory studied in the paper various illustrated examples are presented.

keywords: Biomathematics, Biological growth, Mathematical model, Darboux frame, Quaternion Algebras.

AMS 92*B*99, 74*K*99, 53*A*04.

1 Introduction

In nature, there are a variety of living species, and the most important factor affecting the growth of these organisms is the environment. For example, some living things develop as dependent on another. Therefore, when modeling the growth of such creatures, the effect of the surface on which it is dependent should also be taken into consideration. In this study, we tried to explain these creatures by using the surface-dependent growth model. The most important examples of surface-dependent growth are parasites. The parasites usually have a ring or spiral structure and stick to the surface and live there. One of these parasite species is Liana which given in Figure 5. The liana is a long-stemmed, woody vine that uses trees, as well as other means of vertical support, to climb up to the canopy to get access to well-lit areas of the forest. They begin life on the forest floor but depend on trees for support as they climb upwards towards the sunlight they need for survival. The other one is the Christmas tree parasite. It is believed that this parasite the largest in the world, a tree whose greedy roots stab victims up to 110m away. The Christmas tree (Nuytsia

*Corresponding author. E–mail: sezen.oncul@ankara.edu.tr (S. Öncül)

floribunda) has blades for slicing into the roots of plants to steal their sap. The Christmas tree is indiscriminate, stealing juice from almost anything green – grasses, sedges, carrots, weeds, vines, shrubs, eucalypts. When one of its roots meets another root it forms a collar of tissue around it, like a swollen wedding ring, and a hydraulically operated blade forms inside that. A model for this parasite is shown in Figure 4. Besides, some of these models are shown in nature equivalents. Now let us summarize the studies on surface growth model. The first study to understand the Molluscan shell began with Moseley. The author describes the spiral coils of the Molluscan shell in terms of the mathematical and geometrical aspects [18]. Then, several models and approaches devised by Raup [20, 21], which strengthened the research field called "theoretical morphology". At first, the initial work focused on the shape of the shells [5, 17] and understanding the evolution of the shell form under growth process [12]. Nevertheless, there is no complete understanding of how these structures grow in mathematically. Then, using the complex coordinates Illerts, give a formulation that describes the seashells growth [13]. In addition, in [14], the author formulated the problem of seashell geometry in real space $\mathbb{R}^3$ and obtained equations that could be used for computer simulations. Later, Moulton et al. developed an appropriate mathematical framework, which is not bound to computer algorithms to generate surfaces, to solve this problem [19]. In [24], the authors consider a space curve instead of a planar curve and they define the growth vector field in terms of an alternative moving frame $\{N, C, W\}$ on the generating curve. This frame ideally describes the growth in the direction of the Darboux vector. [25], it is investigated that the time dimension in the method affects the growth of the surfaces. Thus, they determine the model of the growth function in the three-dimensional Minkowski space with timelike and spacelike generating curve.

Quaternions are a non-commutative number system extends the complex numbers. Quaternions and their applications to mechanics were first described by Rodrigues (1840) and Hamilton (1843). Quaternions have important applications in theoretical and applied mathematics. Particularly, they provide great convenience in applications involving three-dimensional rotations. Surfaces can be more easily expressed using quaternions. Many studies on quaternionic representations of surfaces have been achieved [1–3, 6, 9, 15]. These studies have examined quaternionic expressions of surfaces such as constant slope and canal surfaces in Euclidean and Minkowski spaces.

This paper is organized as follows: In Section 2, we give some preliminaries about Darboux frame and quaternion algebra. In Section 3, firstly, the surface-dependent growth model with quaternions and Darboux frame in Euclidean 3-space are introduced and the related growth velocity components are calculated. Also, we present the growth model along the conditions for a curve to be a geodesic, asymptotic, line of curvature and rhumb line on the surface. In Section 3, various illustrated examples, which include various biological model in the nature, are presented. In the last section is devoted to the conclusions and discussions.

2 Preliminaries

Let $\mathbb{R}^3$ be 3-dimensional Riemannian space endoved with the metric is given by

$$\pi(u,v) = u_1v_1 + u_2v_2 + u_3v_3, \tag{1}$$

for $u=(u_1,u_2,u_3)$ and $v=(v_1,v_2,v_3)$. The vector product is

$$u\times v=\begin{vmatrix} e_1 & e_2 & e_3 \\ u_1 & u_2 & u_3 \\ v_1 & v_2 & v_3 \end{vmatrix}. \tag{2}$$

Let $S\subset\mathbb{E}^3$ be an oriented surface and $\gamma: I\subset\mathbb{R}\to S$ be a unit speed curve. Let T denote the unit tangent vector field of γ and N denote the unit normal vector field of the surface S restricted to the curve γ. Then the Darboux frame field along γ is given by $\{T,Y,N\}$ where $Y=N\wedge T$. Thus, we can express the derivatives according to the arc-length parameter s of each vector field along the curve γ as:

$$\begin{bmatrix} T' \\ Y' \\ N' \end{bmatrix}=\begin{bmatrix} 0 & k_g & \kappa_n \\ -k_g & 0 & \tau_g \\ -\kappa_n & -\tau_g & 0 \end{bmatrix}\begin{bmatrix} T \\ Y \\ N \end{bmatrix}, \tag{3}$$

where k_g, κ_n and τ_g denote the geodesic curvature, normal curvature, and geodesic torsion of the curve γ, respectively.
For the curve γ lying on the surface S we have following three cases:
i) γ is a geodesic curve if and only if $k_g=0$,
ii) γ is an asymptotic line if and only if $\kappa_n=0$,
iii) γ is a principal line if and only if $\tau_g=0$ [8].

Quaternions can be defined by the set Q. They defined with following multiplication rules in Q [11].

$$Q=\left\{Q_0+Q_1i+Q_2j+Q_3k, i^2=j^2=-k^2=-1, ij=k=-ji, jk=i=-kj, ki=j=-ik\right\}. \tag{4}$$

The quaternion product of two quaternions $P_0+P_1i+P_2j+P_3k$ and $Q_0+Q_1i+Q_2j+Q_3k$ is defined as

$$PQ=P_0Q_0-\pi(V_P,V_Q)+P_0V_Q+Q_0V_P+V(V_P\times V_Q), \tag{5}$$

where $\pi(V_P,V_Q)$ and $V_P\times V_Q$ are the scalar product and the vector product, respectively. If P and Q are pure, then

$$\begin{aligned} PQ &= -\pi(V_P,V_Q)+V_P\times V_Q \\ &= -(P_1Q_1+P_2Q_2+P_3Q_3)+\begin{vmatrix} i & j & k \\ P_1 & P_2 & P_3 \\ Q_1 & Q_2 & Q_3 \end{vmatrix}. \end{aligned} \tag{6}$$

The quaternion product is given as the form

$$PQ=\begin{bmatrix} P_0 & -P_1 & -P_2 & -P_3 \\ P_1 & P_0 & -P_3 & P_2 \\ P_2 & P_3 & P_0 & -P_1 \\ P_3 & -P_2 & P_1 & P_0 \end{bmatrix}\begin{bmatrix} Q_0 \\ Q_1 \\ Q_2 \\ Q_3 \end{bmatrix}. \tag{7}$$

Conjugate, norm and inverse of the quaternion $Q=Q_0+Q_1i+Q_2j+Q_3k$ are given respectively,

$$\bar{Q}=Q_0-Q_1i-Q_2j-Q_3k, \tag{8}$$

$$N_Q = \sqrt{Q\bar{Q}} = \sqrt{\bar{Q}Q} = \sqrt{Q_0^2 + Q_1^2 + Q_2^2 + Q_3^2}, \tag{9}$$

$$Q^{-1} = \frac{\bar{Q}}{N_Q}. \tag{10}$$

Also, each quaternion $Q = Q_0 + Q_1 i + Q_2 j + Q_3 k$ can be written in the form

$$Q_0 = N_q(\cos\theta + \varepsilon_0 \sin\theta),$$

where $\cos\theta = \frac{Q_0}{N_Q}$, $\sin\theta = \frac{\sqrt{Q_1^2+Q_2^2+Q_3^2}}{N_Q}$, $\varepsilon_0 = \frac{(Q_1,Q_2,Q_3)}{\sqrt{Q_1^2+Q_2^2+Q_3^2}}$, and $\varepsilon_0^2 = -1$ [11].

Theorem 2.1. If $Q = Q_0 + Q_1 i + Q_2 j + Q_3 k = \cos\theta + \varepsilon_0 \sin\theta \in \mathbb{E}^3$, is a quaternion then the linear map $R_\theta(v) = qvq^{-1}$ gives a rotation through the angle 2θ, about the axis ε_0 where $v \in \mathbb{R}^3$. The rotation matrix corresponding to the quaternion q is

$$R_\theta^q = \begin{bmatrix} Q_0^2 + Q_1^2 - Q_2^2 - Q_3^2 & 2Q_1Q_2 - 2Q_0Q_3 & 2Q_1Q_3 + 2Q_0Q_2 \\ 2Q_1Q_2 + 2Q_0Q_3 & Q_0^2 - a_1Q_1^2 + Q_2^2 - Q_3^2 & 2Q_2Q_3 - 2Q_0q1 \\ 2Q_1q_3 - 2Q_0Q_2 & 2Q_2Q_3 + 2Q_0Q_1 & Q_0^2 - Q_1^2 - Q_2^2 + Q_3^2 \end{bmatrix}, \tag{11}$$

where R_θ^q is orthogonal, i.e, $(R_\theta^q)^t R_\theta^q = I$ and $\det(R_\theta^q) = 1$ [23].

3 Surface-dependent Growth Model

The goal of this section is to present the kinematic aspects of surface-dependent growth. Many of the features of plant and parasite growth find their explanation on-within the surface. It is, therefore, useful to focus on the growth of plant and parasite on the surface. The material forms and expansion depends on the shape of the main surfaces. This form of structure grows by adding new material so that one point remains on the surface. For this form evolution, there must be a growth component in the direction of the vector Darboux frame component Y. For this, the growth vector field is defined in terms of the Darboux frame $\{T, Y, N\}$ on the generating curve. This frame ideally describes the surface-dependent growth model.

Definition 3.1. Let $r(s,0) = (r_1(s,0), r_2(s,0))$ be a planar curve. Then the planarity implies that the surface can be expressed as

$$r(s,t) = p(t) + \mu(s,t)\mathbf{d}_3(t) + \nu(s,t)(r_1\mathbf{d}_2 + r_2\mathbf{d}_1), \tag{12}$$

where $p(t)$ is a position vector to a point in the plane of the curve, $\mu(t,s) = -\lambda\dot{\lambda}$, $\nu(t,s) = \pm\lambda\sqrt{1-\dot{\lambda}^2}$ with the scaling $\lambda(s,t)$.

3.2 Accretive Surface-Dependent Growth Model through Quaternions

Theorem 3.3. Let $p(t) : I \subset \mathbb{R} \to \mathbb{R}^3$ be an arc-length curve with the Darboux frame apparatus $\{\mathbf{d}_1, \mathbf{d}_2, \mathbf{d}_3, \kappa_n, k_g, \tau_g\}$. By using the unit quaternion $Q(s,t) = r_1 + r_2\mathbf{d}_3(s)$, we obtain the parametric

equation of the accretive surface:
(i)Pparametric representation with quaternion product $Q(s,\theta)\mathbf{d}_2(t)$,

$$r(s,t) = p(t) + \mu(s,t)\mathbf{d}_3(t) + \nu(s,t)Q(s,t)\mathbf{d}_2(\mathbf{t}). \tag{13}$$

(ii) Parametric representation with homothetic motion

$$r(s,t) = p(t) + \mu(s)\mathbf{t}(t) + \nu(s)R_\theta^q\mathbf{d}_2(\mathbf{t}), \tag{14}$$

where $\mu(s) = -\lambda(s,t)\dot{\lambda}(s,t), \nu(s) = \pm\lambda(s,t)\sqrt{1+\dot{\lambda}(s,t)^2}$, and R_θ^q is the matrix form of the unit quaternion $q(s,t)$.

Proof. Assume that $r(s,t)$ is a surface generated by the arbitrary unit speed curve $p(t)$. Then we have

$$r(s,t) = p(t) + \mu(s,t)\mathbf{d}_3(t) + \nu(s,t)(r_1\mathbf{d}_2 + r_2\mathbf{d}_1).$$

If we use the quaternion product for unit quaternion $Q(s,t) = r_1 + r_2\mathbf{d}_3(s)$ and the pure quaternion $\mathbf{d}_2(\mathbf{s})$, we obtain

$$Q(s,\theta)\times\mathbf{d}_2(\mathbf{s}) = r_1\mathbf{d}_2(\mathbf{s}) + r_2\mathbf{d}_1(\mathbf{s}).$$

Then using the last equation, we reach the surfaces as

$$r(s,t) = p(t) + \mu(s,t)\mathbf{d}_3(t) + \nu(s,t)Q(s,t)\mathbf{d}_2(t)$$

and the matrix representation of the surface given as

$$r(s,t) = p(t) + \mu(s)\mathbf{t}(t) + \nu(s)R_\theta^q\mathbf{d}_2(t),$$

where $\beta(t) = p(t) + \mu(s)\mathbf{d}_3(s)$ is translation vector, $\nu(s)$ is homothetic scalar and R_θ^q orthogonal matrix of the homothetic motion. Therefore, we can say that $r(s,t) = \beta(t) + \nu(s)R_\theta^q\mathbf{d}_2(\mathbf{t})$ is the homothetic motion. These complates the proof.

Example 3.4. Assume that $r(s,t)$ is a surface generated by the unit speed curve $p(t) = (\cos t, \sin t, 1)$ as the line of curvature on the surface $S(u,v) = (u,v,u^2+v^2)$. The Darboux frame and curvatures of the curve $p(t)$ calculated as

$$\begin{aligned}
\mathbf{d}_1 &= (-\frac{2}{\sqrt{5}}\cos t, -\frac{2}{\sqrt{5}}\sin t, \frac{1}{\sqrt{5}}),\\
\mathbf{d}_2 &= (-\frac{1}{\sqrt{5}}\cos t, -\frac{1}{\sqrt{5}}\sin t, -\frac{2}{\sqrt{5}}),\\
\mathbf{d}_3 &= (-\sin t, \cos t, 0),
\end{aligned} \tag{15}$$

,

$$\kappa_n = \frac{2}{\sqrt{5}},\ k_g = \frac{1}{\sqrt{5}},\ \tau_g = 0.$$

Then, using the eqs.(15) into the eq.(14) the surface can be obtained. It is illustrated in Figure 1(a).

Example 3.5. Nex we take $p(t) = (\cos\frac{t}{\sqrt{2}}, \sin\frac{t}{\sqrt{2}}, \frac{t}{\sqrt{2}})$ as a geodesic curve on the surface $S(u,v) = (\cos u, \sin u, v)$ Then the Darboux frame and curvatures of the curve $p(t)$ is obtained as

$$\mathbf{d}_1 = (\cos\frac{t}{\sqrt{2}}, \sin\frac{t}{\sqrt{2}}, 0),$$
$$\mathbf{d}_2 = (\frac{1}{\sqrt{2}}\sin\frac{t}{\sqrt{2}}, -\frac{1}{\sqrt{2}}\cos\frac{t}{\sqrt{2}}, \frac{1}{\sqrt{2}}),$$
$$\mathbf{d}_3 = (-\frac{1}{\sqrt{2}}\sin\frac{t}{\sqrt{2}}, \frac{1}{\sqrt{2}}\cos\frac{t}{\sqrt{2}}, \frac{1}{\sqrt{2}}).$$

$$\kappa_n = -\frac{1}{2},\ k_g = 0,\ \tau_g = \frac{1}{2}.$$

Then the related surface is given in Figure 1(b).

Example 3.6. Now we take $p(t) = (\cos\frac{t}{\sqrt{2}}, \sin\frac{t}{\sqrt{2}}, \frac{t}{\sqrt{2}})$ as a asymptotic curve on the surface $S(u,v) = (v\cos u, v\sin u, u)$. Then the Darboux frame and curvatures of the curve $p(t)$ is obtained as

$$\mathbf{d_1} = (-\frac{1}{\sqrt{2}}\sin\frac{s}{\sqrt{2}}, \frac{1}{\sqrt{2}}\cos\frac{s}{\sqrt{2}}, -\frac{1}{\sqrt{2}}),$$
$$\mathbf{d_2} = (\cos\frac{s}{\sqrt{2}}, -\sin\frac{s}{\sqrt{2}}, 0),$$
$$\mathbf{d_3} = (-\frac{1}{\sqrt{2}}\sin\frac{s}{\sqrt{2}}, \frac{1}{\sqrt{2}}\cos\frac{s}{\sqrt{2}}, \frac{1}{\sqrt{2}}),$$

$$\kappa_n = 0,\ \kappa_g = -\frac{1}{2},\ \tau_g = \frac{1}{2}.$$

Then the related surface growth illustrated in Figure 1(c).

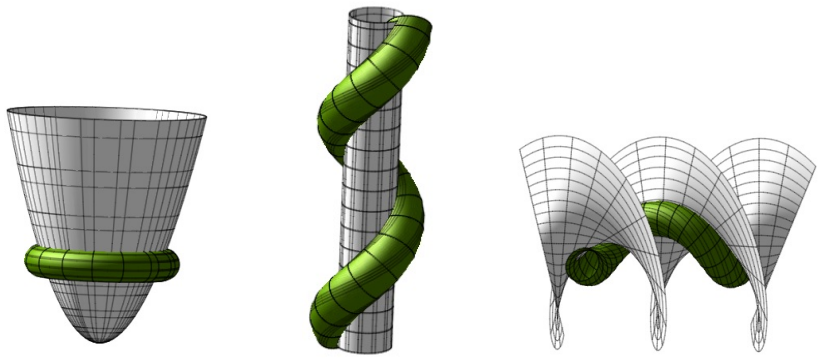

(a) (b) (c)

Figure 1: (a) Growth along a line of curvature, (b) Growth along a geodesic curve, (c) Growth along an asymptotic curve

Note: In this form growth model the surface keeps shape constancy of the curve.

3.7 Growth velocity field of the surface

Theorem 3.8. Let $r(s,0)$ be a curve which is parameterized by arc-length and each point of the generating curve has followed a path in time that has been on the surface. Then the growth velocity components of the accretive surface-dependent growth model obtained as

$$
\begin{aligned}
q_1 &= \frac{(\dot{\nu}r_1 - \mu\kappa_n + \nu r_2\tau_g)((\nu' r_2 + \nu r_2')(1+\dot{\mu} - \nu r_1\kappa_n - \nu r_2 k_g) - (\mu')(\mu k_g + \dot{\nu} r_2 - \nu r_1\tau_g))}{A} \\
&\quad + \frac{(\mu k_g + \dot{\nu} r_2 - \nu r_1\tau_g)((\dot{\nu}r_1 - \mu\kappa_n + \nu r_2\tau_g)(\mu') - (\nu' r_1 + \nu r_1')(1+\dot{\mu} - \nu r_1\kappa_n - \nu r_2 k_g)}{A}), \\
q_2 &= -(\dot{\nu}r_1 - \mu\kappa_n + \nu r_2\tau_g) r_2{}' \frac{(\nu' r_1 + \nu r_1')(\mu k_g + \dot{\nu} r_2 - \nu r_1\tau_g) - (\dot{\nu}r_1 - \mu\kappa_n + \nu r_2\tau_g)(\nu' r_2 + \nu r_2')}{A} \\
&\quad + (\mu k_g + \dot{\nu} r_2 - \nu r_1\tau_g) r_1{}' \frac{-(\nu' r_1 + \nu r_1')(\mu k_g + \dot{\nu} r_2 - \nu r_1\tau_g) - (\dot{\nu}r_1 - \mu\kappa_n + \nu r_2\tau_g)(\nu' r_2 + \nu r_2')}{A} \\
&\quad + (1+\dot{\mu} - \nu r_1\kappa_n - \nu r_2 k_g)(\frac{(r_2'((\nu' r_2 + \nu r_2')(1+\dot{\mu} - \nu r_1\kappa_n - \nu r_2 k_g) - \mu'(\mu k_g + \dot{\nu} r_2 - \nu r_1\tau_g)))}{A} \\
&\quad - r_1'(\frac{(\dot{\nu}r_1 - \mu\kappa_n + \nu r_2\tau_g)(\mu') - (\nu' r_1 + \nu r_1')(1+\dot{\mu} - \nu r_1\kappa_n - \nu r_2 k_g)}{A}), \\
q_3 &= (\dot{\nu}r_1 - \mu\kappa_n + \nu r_2\tau_g) r_1' + (\mu k_g + \dot{\nu} r_2 - \nu r_1\tau_g) r_2',
\end{aligned}
$$

where $A = \|\partial_s r \times \partial_t r\|$ and $\mu(s,t) = -\lambda(s,t)\dot{\lambda}(s,t), \nu(s,t) = \pm\lambda(s,t)\sqrt{1+\dot{\lambda}(s,t)^2}$ are functions related to the stretch factor λ.

Proof. Let us consider an arbitrary unit speed curve $r(s,0) = (r_1(s,0), r_2(s,0), 0)$. Then, to generate surface we take a dressing curve in the plane of $\mathbf{d}_1$ and $\mathbf{d}_2$. In these case, at any time t, the dressing curve can be written as,

$$r(s) = r_1\mathbf{d}_1 + r_2\mathbf{d}_2.$$

Then the surface can be written in the following form

$$r(s,t) = p(t) + \mu(s,t)\mathbf{d}_3(t) + \nu(s,t)(r_1\mathbf{d}_1 + r_2\mathbf{d}_2) \tag{16}$$

where $p(t)$ is a position vector to a point in the plane of the curve, $\mu(t,s) = -\lambda\dot{\lambda}$, $\nu(t,s) = \pm\lambda\sqrt{1-\dot{\lambda}^2}$ with the scaling $\lambda(s,t)$. Now, we can determine the growth velocity field as

$$\partial_t r = q_1 d_1 + q_2 d_2 + q_3 d_3 \tag{17}$$

where d_i, $i = 1,2,3$ are the local basis for the dressing curve. Then the velocity components of the dressing curve are given as,

$$
\begin{aligned}
q_1 &= B(\partial_t r, d_1), \\
q_2 &= B(\partial_t r, d_2), \\
q_3 &= B(\partial_t r, d_3).
\end{aligned} \tag{18}
$$

If we consider the Frenet frame $\mathbf{d}_i$, $i = 1,2,3$ of the curve $p(t)$ and the case $\partial_t p = \mathbf{d}_3$ then we have,

$$
\begin{bmatrix} \dot{\mathbf{d}}_1 \\ \dot{\mathbf{d}}_2 \\ \dot{\mathbf{d}}_3 \end{bmatrix} = \begin{bmatrix} 0 & -\tau_g & -\kappa_n \\ \tau_g & 0 & -\kappa_g \\ -\kappa_n & \kappa_g & 0 \end{bmatrix} \begin{bmatrix} \mathbf{d}_1 \\ \mathbf{d}_2 \\ \mathbf{d}_3 \end{bmatrix}. \tag{19}
$$

By taking the derivative of the eq. (16) with respect to t, and s, respectively, we calculate

$$\partial_t r(s,t) = (\dot{\nu} r_1 - \mu\kappa_n + \nu r_2\tau_g)\mathbf{d}_1 + (\mu k_g + \dot{\nu} r_2 - \nu r_1\tau_g)\mathbf{d}_2 + (1+\dot{\mu} - \nu r_1\kappa_n - \nu r_2 k_g)\mathbf{d}_3, \quad (20)$$

$$\partial_s r(s,t) = (\nu' r_1 + \nu r_1')\mathbf{d}_1 + (\nu' r_2 + \nu r_2')\mathbf{d}_2 + \mu'\mathbf{d}_3. \quad (21)$$

On the other hand the Darboux frame of the unit speed dressing curve defined via the director vectors as,

$$\begin{aligned} d_1 &= \frac{\partial_s r \times \partial_t r}{\|\partial_s r \times \partial_t r\|}, \\ d_2 &= V(d_1 \times d_3) \\ d_3 &= \frac{\partial_s r}{\|\partial_s r\|_B} = r_1'\mathbf{d}_1 + r_2'\mathbf{d}_2. \end{aligned} \quad (22)$$

Then we compute that

$$\begin{aligned} d_1 &= \frac{(\nu' r_2 + \nu r_2')(1+\dot{\mu} - \nu r_1\kappa_n - \nu r_2\kappa_g) - (\mu')(\mu\kappa_g + \dot{\nu} r_2 - \nu r_1\tau_g)}{A}\mathbf{d}_1, \\ &+ \frac{(\dot{\nu} r_1 - \mu\kappa_n + \nu r_2\tau_g)(\mu') - (\nu' r_1 + \nu r_1')(1+\dot{\mu} - \nu r_1\kappa_n - \nu r_2\kappa_g)}{A}\mathbf{d}_2 \\ &+ \frac{(\nu' r_1 + \nu r_1')(\mu\kappa_g + \dot{\nu} r_2 - \nu r_1\tau_g) - (\dot{\nu} r_1 - \mu\kappa_n + \nu r_2\tau_g)(\nu' r_2 + \nu r_2')}{A}\mathbf{d}_3 \\ d_2 &= -r_2\prime\frac{(\nu' r_1 + \nu r_1')(\mu\kappa_g + \dot{\nu} r_2 - \nu r_1\tau_g) - (\dot{\nu} r_1 - \mu\kappa_n + \nu r_2\tau_g)(\nu' r_2 + \nu r_2')}{A}\mathbf{d}_1 \\ &+ r_1\prime\frac{-(\nu' r_1 + \nu r_1')(\mu\kappa_g + \dot{\nu} r_2 - \nu r_1\tau_g) - (\dot{\nu} r_1 - \mu\kappa_n + \nu r_2\tau_g)(\nu' r_2 + \nu r_2')}{A}\mathbf{d}_2 \\ &+ (\frac{(r_2'((\nu' r_2 + \nu r_2')(1+\dot{\mu} - \nu r_1\kappa_n - \nu r_2\kappa_g) - (\mu')(\mu\kappa_g + \dot{\nu} r_2 - \nu r_1\tau_g)))}{A} \\ &- r_1'(\frac{(\dot{\nu} r_1 - \mu\kappa_n + \nu r_2\tau_g)(\mu') - (\nu' r_1 + \nu r_1')(1+\dot{\mu} - \nu r_1\kappa_n - \nu r_2\kappa_g)}{A})\mathbf{d}_3 \\ d_3 &= \frac{\partial_s r}{\|\partial_s r\|_B} = r_1'\mathbf{d}_1 + r_2'\mathbf{d}_2, \end{aligned} \quad (23)$$

where $A = \|\partial_s r \times \partial_t r\|$.

By substituting d_1, d_2 and d_3 in the eq. (14), we get

$$
\begin{aligned}
q_1 &= \frac{(\dot{\nu} r_1 - \mu\kappa_n + \nu r_2\tau_g)((\nu' r_2 + \nu r_2')(1+\dot{\mu} - \nu r_1\kappa_n - \nu r_2\kappa_g) - (\mu')(\mu\kappa_g + \dot{\nu} r_2 - \nu r_1\tau_g))}{A} \\
&+ \frac{(\mu\kappa_g + \dot{\nu} r_2 - \nu r_1\tau_g)((\dot{\nu} r_1 - \mu\kappa_n + \nu r_2\tau_g)(\mu') - (\nu' r_1 + \nu r_1')(1+\dot{\mu} - \nu r_1\kappa_n - \nu r_2\kappa_g)}{A}) \\
q_2 &= -(\dot{\nu} r_1 - \mu\kappa_n + \nu r_2\tau_g) r_2\prime \frac{(\nu' r_1 + \nu r_1')(\mu\kappa_g + \dot{\nu} r_2 - \nu r_1\tau_g) - (\dot{\nu} r_1 - \mu\kappa_n + \nu r_2\tau_g)(\nu' r_2 + \nu r_2')}{A} \\
&+ (\mu\kappa_g + \dot{\nu} r_2 - \nu r_1\tau_g) r_1\prime \frac{-(\nu' r_1 + \nu r_1')(\mu\kappa_g + \dot{\nu} r_2 - \nu r_1\tau_g) - (\dot{\nu} r_1 - \mu\kappa_n + \nu r_2\tau_g)(\nu' r_2 + \nu r_2')}{A} \\
&+ (1+\dot{\mu} - \nu r_1\kappa_n - \nu r_2\kappa_g)(\frac{(r_2'((\nu' r_2 + \nu r_2')(1+\dot{\mu} - \nu r_1\kappa_n - \nu r_2\kappa_g) - (\mu')(\mu\kappa_g + \dot{\nu} r_2 - \nu r_1\tau_g)))}{A} \\
&- r_1'(\frac{(\dot{\nu} r_1 - \mu\kappa_n + \nu r_2\tau_g)(\mu') - (\nu' r_1 + \nu r_1')(1+\dot{\mu} - \nu r_1\kappa_n - \nu r_2\kappa_g)}{A}) \\
q_3 &= (\dot{\nu} r_1 - \mu\kappa_n + \nu r_2\tau_g) r_1' + (\mu\kappa_g + \dot{\nu} r_2 - \nu r_1\tau_g) r_2',
\end{aligned}
$$

Next we give following corollaries without of proof.

Corollary 3.9. *Let $r(s,0)$ be a curve which is parameterized by arc-length and each point of the generating curve has followed a path in time that has been on the surface. The growth velocity components of the surface $r(s,t) = p(t) + \lambda(s)(r_1\mathbf{d}_1 + r_2\mathbf{d}_2)$ with respect to the Darboux frame obtained as follows*

$$
\begin{aligned}
q_1 &= \frac{(\lambda r_2\tau_g)(\lambda' r_2 + \lambda r_2')(1 - \lambda r_1\kappa_n - \lambda r_2 k_g) - (\lambda' r_1 + \lambda r_1')(1 - \lambda r_1\kappa_n - \lambda r_2 k_g)}{A}, \\
q_2 &= -(\lambda r_2\tau_g) r_2\prime \frac{(\lambda' r_1 + \lambda r_1')(-\lambda r_1\tau_g) - (\lambda r_2\tau_g)(\lambda' r_2 + \lambda r_2')}{A} \\
&+ (-\lambda r_1\tau_g) r_1\prime \frac{-(\lambda' r_1 + \lambda r_1')(-\lambda r_1\tau_g) - (\lambda r_2\tau_g)(\lambda' r_2 + \lambda r_2')}{A} \\
&+ (1 - \lambda r_1\kappa_n - \lambda r_2\kappa_g) \frac{(r_2'\lambda' r_2 + \lambda r_2')(1 - \lambda r_1\kappa_n - \lambda r_2\kappa_g)}{A} \\
&+ \frac{r_1'(\lambda' r_1 + \lambda r_1')(1 - \lambda r_1\kappa_n - \lambda r_2\kappa_g)}{A}, \\
q_3 &= \lambda r_2\tau_g r_1' - \nu r_1\tau_g r_2',
\end{aligned}
$$

where $A = \|\partial_s r \times \partial_t r\|$ and $\lambda(s) = \pm\nu(s,t)$.

3.10 Surface-Dependent Growth Model with Growth Velocity and Darboux Frame Fields

Suppose that at time $t = 0$, we get the generating curve $r(s,0) : [0,I] \to \mathbb{R}^3$ defined for a material parameter s. The surface accretion is modeled via local direction $q(s,0)$ and the rate of growth at each point s. In addition, growth velocity field $q(s,t)$ is defined at each material point s at time t. The growth velocity field $q(s,t)$ directs the evolution of the generating curve $r(s,0)$ and defines a surface $r(s,t)$. This surface is thrice differentiable in the parameter s and t. The curve $r(s_0,t)$ along time t and for a fixed $s = s_o$ will be referred to as a cell track. The velocity vector can be a function

of the local geometry as well as possible physical, chemical, or biological fields (rate of accretion, morphogen gradient, temperature, pH, etc ...) [19].

In order to describe the velocity locally, we attach to the curve $r(s,0)$ a local orthonormal Darboux frame $\{d_1, d_2, d_3\}$. Then the unit tangent vector field defined as,

$$r' \equiv \partial_s r(s,t) = Dv = \lambda d_3, \tag{24}$$

where we use the Euclidean product $Dv = v_1 d_1 + v_2 d_2 + v_3 d_3$, $v \in \mathbb{E}^3$ and $\lambda = (0,0,\lambda)$ describes the stretch of the curve with respect to the initial arc length expressed in the local frame.

The derivations of the frame for the parameters s and t can be given as,

$$D' \equiv \partial_s D = DU, \tag{25}$$
$$\dot{D} \equiv \partial_t D = DW,$$

where U and W are the Darboux matrices in $\mathbb{E}^3$ defined as

$$U := \begin{bmatrix} 0 & -u_3 & u_2 \\ u_3 & 0 & -u_1 \\ -u_2 & u_1 & 0 \end{bmatrix} \text{ and } W := \begin{bmatrix} 0 & -w_3 & w_2 \\ w_3 & 0 & -w_1 \\ -w_2 & w_1 & 0 \end{bmatrix}. \tag{26}$$

If we use the generating curve and its attached basis, then we can write the velocity vector $q(s,t)$ through the local frame as follows,

$$\dot{r}(s,t) = \partial_t r = q(s,t) = Dq, \tag{27}$$

where $q = (q_1, q_2, q_3)$ is the velocity expressed in the local frame. Since the general basis of D is orthonormal (*i.e*, $D^T D = 1$), we have

$$\begin{aligned} q' - \dot{\lambda} &= W\lambda - Uq, \\ W' - U^{\cdot} &= UW - WU. \end{aligned} \tag{28}$$

The Darboux matrix U takes the form,

$$U = \lambda \begin{bmatrix} 0 & -\tau_g & -\kappa_n \\ \tau_g & 0 & -\kappa_g \\ \kappa_n & \kappa_g & 0 \end{bmatrix},$$

which is providing a structure for the growth velocity and solving the system.

The Darboux derivative formulas can be written as:

$$\begin{bmatrix} d_1' \\ d_2' \\ d_3' \end{bmatrix} = \begin{bmatrix} 0 & -\tau_g & -\kappa_n \\ \tau_g & 0 & -\kappa_g \\ -\kappa_n & \kappa_g & 0 \end{bmatrix} \begin{bmatrix} d_1 \\ d_2 \\ d_3 \end{bmatrix}. \tag{29}$$

If the equations are rewritten in terms of the components, then the eq.(11) and eq.(29) gives us a set of six nonlinear first order partial differential equations for a given velocity vector q.

$$\begin{aligned} q_1' - \kappa_n q_3 - \tau_g q_2 &= \lambda w_2, \\ q_2' + \tau_g q_1 - \kappa_g q_3 &= -\lambda w_1, \\ q_3' + \kappa_g q_2 + \kappa_n q_1 &= \dot{\lambda}, \\ -w_1' &= -\kappa_n w_3 - \tau_g w_2, \\ -w_2' &= \tau_g w_1 - \kappa_g w_3, \\ -w_3' &= k_g w_2 - \kappa_n w_1. \end{aligned}$$

In these situations, we can give the following theorem without proof.

Theorem 3.11. (**Main theorem**) The growth of a surface from a generating curve with respect to Darboux frame satisfy the following differential systems:

$$\begin{aligned} q_1' - \kappa_n q_3 - \tau_g q_2 &= \lambda w_2, \\ q_2' + \tau_g q_1 - \kappa_g q_3 &= -\lambda w_1, \\ q_3' + \kappa_g q_2 + \kappa_n q_1 &= \dot{\lambda}, \\ -w_1' &= -\kappa_n w_3 - \tau_g w_2, \\ -w_2' &= \tau_g w_1 - \kappa_g w_3, \\ -w_3' &= k_g w_2 - \kappa_n w_1. \end{aligned} \tag{30}$$

For a given growth velocity, the local frame on the generating curve is freely chosen and the system is solved. After then the surfaces is obtained by the integrating the equation $\partial_t r(s,t) = Dq$.

4 Examples

Fist, we choose the dressing curve as a curve parameterized as $r(s,0) = ((1+0.12\cos 10s)\cos s, (1+0.12\cos 10s)\sin s, 0)$. Then the component of the growth velocity obtained as follows

$$\begin{aligned} q_1 &= \frac{-(\lambda r_1')(1+\lambda r_1 - \lambda r_2 k_g)}{A}, \\ q_2 &= (1+\lambda r_1 - \lambda r_2 \kappa_g)\frac{(r_2'\lambda' r_2 + \lambda r_2')(1+\lambda r_1 - \lambda r_2 \kappa_g)}{A} \\ &\quad + \frac{r_1'(\lambda' r_1 + \lambda r_1')(1+\lambda r_1 - \lambda r_2 \kappa_g)}{A}, \\ q_3 &= 0, \end{aligned}$$

where $r_1 = (1+0.12\cos 10s)\cos s$ and $r_2 = (1+0.12\cos 10s)\sin s$. The surfaces are obtained by integrating $\partial_t r(s,0) = Dq$ or using the quaternion $Q = Q_0 + Q_1 i + Q_2 j + Q_3 k$ in Theorem 4.

The components of the quaternion Q computed as in the following forms: For surface growth along the helices on the sphere,

$$\begin{aligned} Q_0 &= \frac{(1+0.12\cos 10t)\cos t}{A} \\ Q_1 &= -\frac{(1+0.12\cos 10t)\sin t(\sin\frac{s}{c}(b^2-s^2)+\cos\frac{s}{c}sc)}{A}, \\ Q_2 &= -\frac{(1+0.12\cos 10t)\sin t(\cos\frac{s}{c}(-b^2+s^2+sc)+\sin\frac{s}{c}sc))}{A}, \\ Q_3 &= \frac{(1+0.12\cos 10t)\sin t}{A}, \end{aligned}$$

where $A = \sqrt{(\frac{b^4+b^2c^2-2b^2s^2+s^4}{(b^2s^2)c^2})}$ and $b, c \in \mathbb{R}$.

For surface growth along the rhumb lines of the sphere,

$$
\begin{aligned}
Q_0 &= \frac{(1+0.12\cos 10t)\cos t}{B},\\
Q_1 &= \frac{(1+0.12\cos 10t)\sin t(\cos s\sinh(ks)+\sin s\cosh(ks))}{B},\\
Q_2 &= -\frac{(1+0.12\cos 10t)\sin t(\sin s\sinh(ks)-\cos s\cosh(ks))}{B},\\
Q_3 &= \frac{(1+0.12\cos 10t)k\sin t}{B},
\end{aligned}
$$

where $B=\cosh(ks)\sqrt{(k^2+1)}$ and $k\in\mathbb{R}$. The surfaces are illustrated in Figure 2.

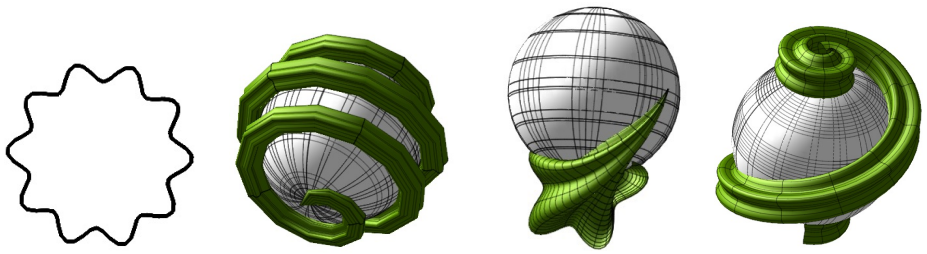

(a) (b) (c) (d)

Figure 2: (a) The cross-section of the curves on the sphere, (b) Surface growth along a helix on the sphere with $\lambda=0.25$, (c) Surface growth along a rhumb line of the sphere with $\lambda=0.25s$, (d) Surface growth along the rhumb lines of the sphere with $\lambda=0.25$.

In the following examples we take the dressing curve as a circle for easier calculation. First we determine the growth velocity and

Example 4.1. Next we choose the dressing curve as a circle parameterized as $r(s,0)=(\cos s,\sin s,0)$ and the center of the circle traces out the curve $p(t)$ on the 2D sphere. Then the growth velocity components calculated as

$$
\begin{aligned}
q_1 &= \frac{(\lambda\sin s)(1+\lambda\cos s-\lambda\sin s\kappa_g)}{A},\\
q_2 &= (1+\lambda\cos s-\lambda\sin s\kappa_g)\frac{(\cos s\lambda'\sin s+\lambda\cos s)(1+\lambda\cos s-\lambda\sin s\kappa_g)}{A}\\
&\quad+\frac{-\cos s(\lambda'\cos s-\lambda\sin s)(1+\lambda\cos s-\lambda\sin s\kappa_g)}{A},\\
q_3 &= 0,
\end{aligned}
$$

The surfaces are obtained by integrating $\partial_t r(s,0)=Dq$ or using the quaternion $Q=Q_0+Q_1 i+Q_2 j+Q_3 k$ in Theorem 4. The components of the quaternion Q computed as in the following

forms: For growth along a circle

$$
\begin{aligned}
Q_0 &= \frac{\cos t}{A},\\
Q_1 &= \frac{\sin t(\sin(\cos s)\sin s\sin(\sin s)+\cos(\cos s)\cos(\sin s)\cos s)}{A},\\
Q_2 &= \frac{\sin t(\sin(\cos s)\sin s\cos(\sin s)-\cos(\cos s)\sin(\sin s)\cos s)}{A},\\
Q_3 &= -\frac{\sin t\cos(\cos s)\sin s}{A},
\end{aligned}
$$

where $A=\sqrt{(}\frac{\cos^2(\frac{\cos s}{2})\cos^2 s-\cos^2 s+1}{2})$. For growth along a spiral,

$$
\begin{aligned}
Q_0 &= \frac{\cos t}{A}\\
Q_1 &= \frac{-\sin t(-\sin(FresnelC(s))\cos^2(\frac{\pi s^2}{2})\sin(FresnelS(s)))}{A}\\
&\quad+\frac{\cos(FresnelC(s))\sin^2(\frac{\pi s^2}{2})\cos(FresnelS(s)))}{A},\\
Q_2 &= \frac{-\sin t(-\sin(FresnelC(s))\cos^2(\frac{\pi s^2}{2})\cos(FresnelS(s)))}{A}\\
&\quad-\frac{\cos(FresnelC(s))\sin^2(\frac{\pi s^2}{2})\sin(FresnelS(s)))}{A},\\
Q_3 &= -\frac{\sin t\cos(FresnelC(s))\cos^2(\frac{\pi s^2}{2})}{A},
\end{aligned}
$$

where $A=\sqrt{(}-\cos^2(FresnelC(s))\cos^2(\frac{\pi s^2}{2})+\cos^2(FresnelC(s))+\cos^2(\frac{\pi s^2}{2}))$.

For growth along a helix,

$$
\begin{aligned}
Q_0 &= \frac{\cos t}{A},\\
Q_1 &= -\frac{\sin t(\sin\frac{s}{c}(b^2-s^2)+\cos\frac{s}{c}sc)}{A},\\
Q_2 &= -\frac{\sin t(\cos\frac{s}{c}(-b^2+s^2+sc)+\sin\frac{s}{c}sc))}{A},\\
Q_3 &= \frac{\sin t}{A},
\end{aligned}
$$

where $A=\sqrt{(}\frac{b^4+b^2c^2-2b^2s^2+s^4}{(b^2s^2)c^2})$ and $b,c\in\mathbb{R}$. The surfaces are illustrated in Figure 3.

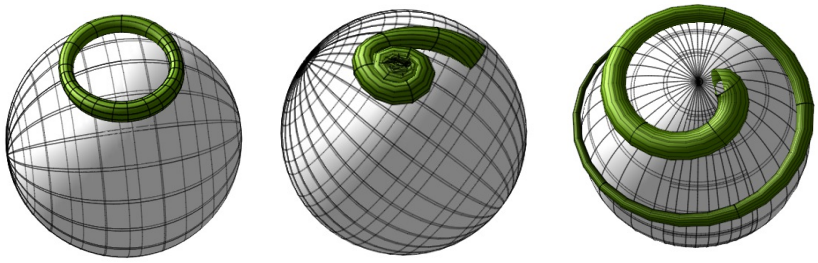

(a) (b) (c)

Figure 3: (a) Growth along a circle, (b) Growth along a spiral, (c) Growth along a helix.

Example 4.2. Next, we choose the dressing curve as a circle parameterized as $r(s,0) = (\cos s, \sin s, 0)$ and the center of the circle traces out the curve $p(t)$ on the 2D torus.

$$
\begin{aligned}
q_1 &= \frac{(\lambda \sin s\tau_g)(\lambda' \sin s + \lambda \cos s)(1 - \lambda \cos s\kappa_n - \lambda \sin s\kappa_g)}{A} \\
&\quad - \frac{(\lambda' \cos s - \lambda \sin s)(1 - \lambda \cos s\kappa_n - \lambda \sin s\kappa_g)}{A}, \\
q_2 &= -(\lambda \sin s\tau_g)\cos s \frac{(\lambda' \cos s - \lambda \sin s)(-\lambda \cos s\tau_g) - (\lambda \sin s\tau_g)(\lambda' \sin s + \lambda \cos s)}{A} \\
&\quad - (-\lambda \cos s\tau_g)\sin s \frac{-(\lambda' \cos s - \lambda \sin s)(-\lambda \cos s\tau_g) - (\lambda \sin s\tau_g)(\lambda' \sin s + \lambda \cos s)}{A} \\
&\quad + (1 - \lambda \cos s\kappa_n - \lambda \sin s\kappa_g) \frac{(\cos s\lambda' \sin s + \lambda \cos s)(1 - \lambda \cos s\kappa_n - \lambda \sin s\kappa_g)}{A} \\
&\quad - \frac{\sin s(\lambda' \cos s - \lambda \sin s)(1 - \lambda \cos s\kappa_n - \lambda \sin sk_g)}{A}, \\
q_3 &= -\lambda \sin s\tau_g \sin s - \nu \cos s\tau_g \cos s.
\end{aligned}
$$

In these cases, the surface is obtained by integrating $\partial_t r(s,0) = Dq$ or using the quaternion $Q = Q_0 + Q_1 i + Q_2 j + Q_3 k$ in Theorem 4. The components of the quaternion Q computed as in the following forms:

$$
\begin{aligned}
Q_0 &= \frac{\cos t}{A}, \\
Q_1 &= -\sin t \sin s, \\
Q_2 &= 0, \\
Q_3 &= -\sin t \cos s,
\end{aligned}
$$

For growth along a spiral,

$$
\begin{aligned}
Q_0 &= \frac{\cos t}{A},\\
Q_1 &= \frac{\sin t(-\sin(FresnelC(s))\cos(\frac{\pi s^2}{2})\cos(FresnelS(s)))}{A}\\
&\quad - \frac{\sin(FresnelS(s))\sin(\frac{\pi s^2}{2})\cos(FresnelC(s))) - 2\sin(FresnelS(s))\sin(\frac{\pi s^2}{2})}{A},\\
Q_2 &= \frac{-\sin t(-\sin(FresnelC(s))\cos(\frac{\pi s^2}{2})\sin(FresnelS(s)))}{A}\\
&\quad - \frac{+\cos(FresnelS(s))\sin(\frac{\pi s^2}{2})\cos(FresnelC(s))) + 2\cos(FresnelS(s))\sin(\frac{\pi s^2}{2})}{A},\\
Q_3 &= \frac{\sin t\cos(FresnelC(s))\cos(\frac{\pi s^2}{2})}{A},
\end{aligned}
$$

where $A = \sqrt{(}-\cos^2(FresnelC(s))\cos^2(\frac{\pi s^2}{2}) + \cos^2(FresnelC(s)) + \cos^2(\frac{\pi s^2}{2}))$.

For growth along an arbitray curve,

$$
\begin{aligned}
Q_0 &= \frac{\cos t}{A},\\
Q_1 &= -\frac{\sin t(\sin(as)a\cos(ps) + \sin(ps)p\cos(as) + 2\sin(ps)p)}{A},\\
Q_2 &= -\frac{\sin t(-\cos(as)a\cos(ps) + \sin(ps)p\sin(as) - 2\cos(ps)p)}{A},\\
Q_3 &= \frac{\sin t\cos(as)a}{A},
\end{aligned}
$$

where $A = \sqrt{(}\cos^2(as)p^2 + 4cos(as)p^2 + a^2 + 4p^2)$ and $b, c \in \mathbb{R}$. The surfaces are illustrated in Figure 4.

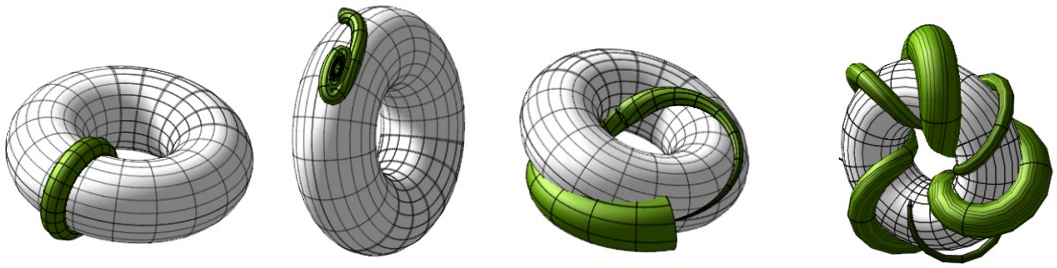

(a) (b) (c) (d)

Figure 4: Surfaces model for growth on the torus.

In the following figures we give various models for surface-dependent growth models in the nature.

$$
\begin{aligned}
q_1 &= \frac{(\lambda \sin s)(1+\lambda\cos s-\lambda \sin s\kappa_g)}{A},\\
q_2 &= (1+\lambda\cos s-\lambda\sin s\kappa_g)\frac{(\cos s\lambda' \sin s+\lambda\cos s)(1+\lambda\cos s-\lambda\sin s\kappa_g)}{A}\\
&\quad+\frac{-\cos s(\lambda'\cos s-\lambda\sin s)(1+\lambda\cos s-\lambda\sin s\kappa_g)}{A},\\
q_3 &= 0,
\end{aligned}
$$

$$
\begin{aligned}
Q_0 &= \frac{\cos t}{A},\\
Q_1 &= -\frac{\sin t(\sin\frac{s}{c}(b^2-s^2)+\cos\frac{s}{c}sc)}{A},\\
Q_2 &= -\frac{\sin t(\cos\frac{s}{c}(-b^2+s^2+sc)+\sin\frac{s}{c}sc))}{A},\\
Q_3 &= \frac{\sin t}{A},
\end{aligned}
$$

where $A=\sqrt{(\frac{b^4+b^2c^2-2b^2s^2+s^4}{(b^2s^2)c^2})}$ and $b,c\in\mathbb{R}$.

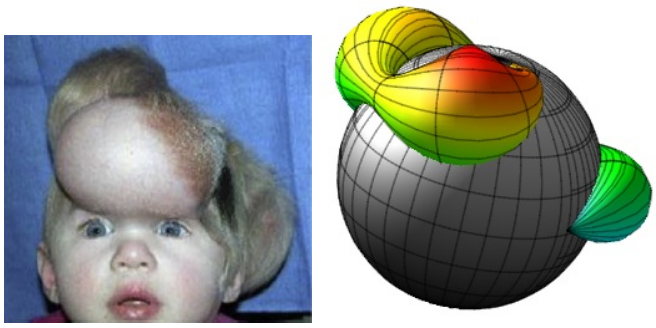

(a) (b)

Figure 5: (a).Tissue expansion in pediatric forehead reconstruction. It shows forehead, anterior and posterior scalp expansion to trigger skin growth in situ [4, 10]. Computational simulation of transversely isotropic area growth predicts area growth in response to controlled mechanical overstretch during tissue expansion [28, 29]. (b) A geometric model for isotropic area growth, for $c=0.40$, $b=3$, and $r=0.5\sin(6s)+0.5s$.

$$
\begin{aligned}
Q_0 &= \cos t,\\
Q_1 &= \sin t(\sqrt{2}\cos^2 s\sin 1 - \frac{\sqrt{2}}{2}\sin 1 + 2\cos 1\sin s\cos s),\\
Q_2 &= \sin t(-\sqrt{2}\cos^2 s\cos 1 + \frac{\sqrt{2}}{2}\cos 1 + 2\sin 1\sin s\cos s),\\
Q_3 &= \sin t(\frac{\sqrt{2}}{2})(2\cos^2 -1).
\end{aligned}
$$

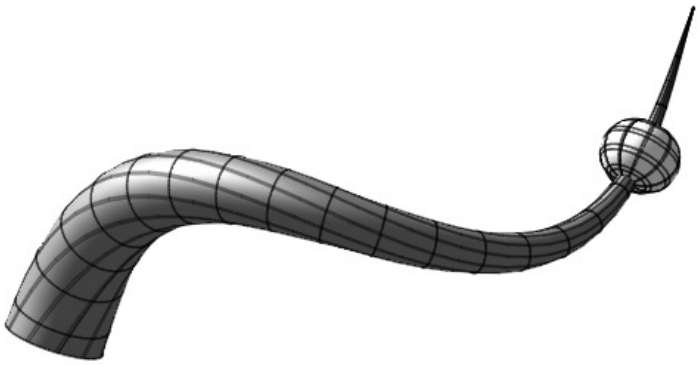

Figure 6: A Christmas tree parasite model.

$$
\begin{aligned}
Q_0 &= \cos t,\\
Q_1 &= -\frac{1}{\sqrt{2}}\sin t\sin s,\\
Q_2 &= \frac{1}{\sqrt{2}}\sin t\cos s,\\
Q_3 &= \frac{1}{\sqrt{2}}\sin t.
\end{aligned}
$$

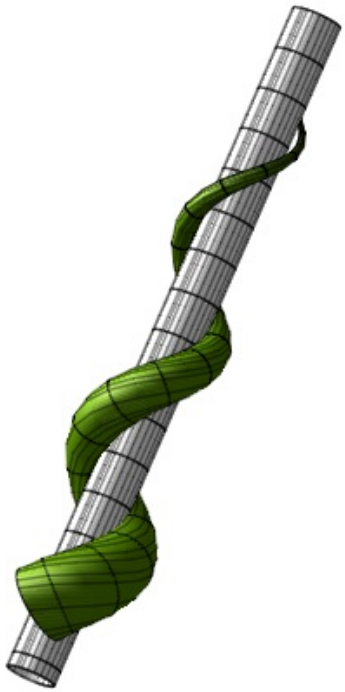

Figure 7: A growth model of the Liana parasite on the tree.

$$Q_0 = \frac{\cos t}{A},$$
$$Q_1 = \frac{\sin t(2\exp -(\cos s+\sin s)((\sin s-\cos s)(\sin(\sin s+\cos s))-(\sin s+\cos s)\cos(\sin s+\cos s))}{A},$$
$$Q_2 = \frac{\sin t(2\exp(\cos s+\sin s)((\sin s-\cos s)(\sin(\sin s+\cos s))+(\sin s-\cos s)\cos(\sin s+\cos s))}{A},$$
$$Q_3 = 0,$$

where $A = 2\sqrt{2\exp 2(\cos s-\sin s)}$

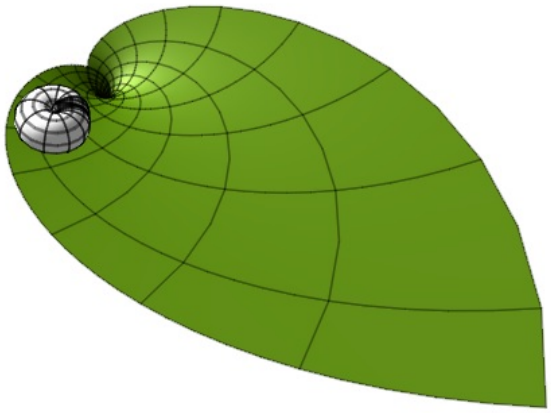

Figure 8: A leaf tree parasite model.

$$
\begin{aligned}
Q_0 &= t\frac{\cos t}{A},\\
Q_1 &= -t^2\frac{\sin t(\sin\frac{s}{c}(b^2-s^2)+\cos\frac{s}{c}sc)}{A},\\
Q_2 &= -t^2\frac{\sin t(\cos\frac{s}{c}(-b^2+s^2+sc)+\sin\frac{s}{c}sc))}{A},\\
Q_3 &= t^2\frac{\sin t}{A},
\end{aligned}
$$

where $A=\sqrt{(\frac{b^4+b^2c^2-2b^2s^2+s^4}{(b^2s^2)c^2})}$ and $b,c\in\mathbb{R}$.

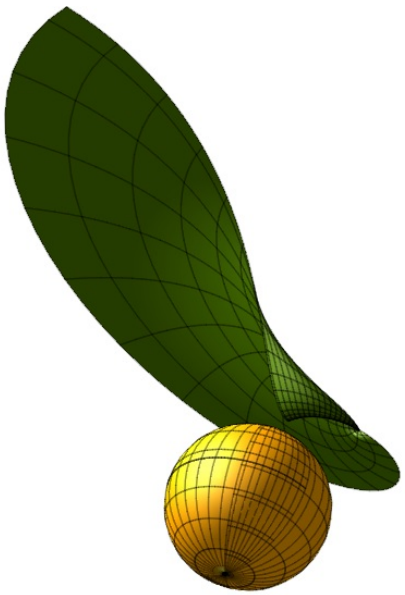

Figure 9: An Oak Apple Gall parasite model.

5 Conclusions and Discussions

Generally, the development of the cancer cell, cysts, tumor, etc. are governed by the anatomy of their surface. These creatures form depending on the surface and the surface controls the accumulation of new material of the parasite. Thus, it may be useful to consider the surface-dependent model when modeling the growth process of these creatures. In this study, the growth kinematics of the different creatures such as parasites, cancer cell, cysts, tumor, etc. are obtained by applying the surface-dependent growth model. In light of these models, generally, we can say that these creatures wrap the surface along the geodesic curves. For example, the geodesics of the cylinder surface are the main lines of the cylinder, circular helices, and circles. If we consider the trunk of a tree as a cylinder, it is seen that some parasites species prefer one of these geodesics. For example, a green vine prefers the main lines of the cylinder, the Liana prefers the helices of the cylinder and the Christmas tree parasite prefers the circle of the cylinder. When we examine nature, it can be examined whether these parasites grow along different curves of the surface such as asymptotic curve, line of curvature and rhumb line. Some images relating to these biological families are given as follows: In Figure 6, we give a model for Christmas tree parasite and in Figure 8 we give a model for the leaf tree parasites. Also, this form of toroidal parasite called chelonibia testudinaria can be seen on the shell surface of the tortoise. In Figure 9 we present a model for an Oak Apple Gall parasite, . Also, the other this form (spherical form parasites) of parasites are leaf parasite, cancer cell, cysts, tumor, etc. In Figure 5 and Figure 7, we give helical parasite model. Figure 5 gives a geometric model for isotropic area growth and Figure 7 gives a model for Liana parasite.

References

[1] S. Aslan and Y. Yaylı, Canal surfaces with quaternions, Adv. Appl. Clifford Algebras 26 (2016) 31ñ38, doi:10.1007/s00006-015-0602-5

[2] S. Aslan and Y. Yaylı, Split quaternions and canal surfaces in Minkowski 3-space, Int. J. Geom. 5(2) (2016) 51ñ61.

[3] M. Babaarslan and Y. Yaylı, A new approach to constant slope surfaces with quaternion, ISRN Geom. 2012 (2012), Article ID: 126358, 8 pp., doi:10.5402/2012/126358.

[4] Buganza Tepole, A., Ploch, C.J., Wong, J., Gosain, A.K., Kuhl, E., 2011. Growin skin: a computational model for skin expansion in reconstructive surgery. J. Mech. Phys. Solids 59, 2177–2190.

[5] A.N Boettiger, G. Oster, Emergent complexity in simple neural systems, Commun Integr Biol. Nov-Dec, **2(6)**(2009), 467-470.

[6] Z. Çanakçı, O. O. Tuncer, I.Gök and Y. Yaylı, The construction of circular · surfaces with quaternions, Asian-European Journal of Mathematics Vol. 12, No. 1 (2019) 1950091 (14 pages), World ScientiÖc Publishing Company doi: 10.1142/S1793557119500918.

[7] P. J. Davis, The Schwarz Function and its Applications, Carius Monograph 17, Mathematical Association of America, (1974).

[8] do Carmo, M.P. Differential geometry of curves and surfaces, Prentice-Hall, Inc. Englefood Cliffs, New Jersey, (1976).

[9] I. Gök, Quaternionic approach of canal surfaces constructed by some new ideas, Adv. Appl. Clifford Algebras 27 (2017) 1175ñ1190, doi:10.1007/s00006-016-0703-9.

[10] Gosain, A.K., Cortes, W., 2007. Pediatric tissue expansion for forehead reconstruction: a 13-year review and an algorithmfor its use.Am. Soc. Plast Surg. Baltimore, Abstract 13288.

[11] Hamilton, W.R.: On Quaternions; or on a new system of imaginaries in algebra. Lond. Edinb. Dublin. Philos. Mag. J. Sci. 25(3), 489–495 (1844)

[12] Ø. Hammer, H. Bucher, Models for the morphogenesis of the molluscan shell, int. J. Paleont. Str. **38**(2)(2005), 111-122.

[13] C. Illert, Formulation and solution of the classical problem, I Seashell geometry, Nuovo Cimento, **9**(7)(1987), 791-814.

[14] C. Illert, Formulation and solution of the classical problem, II Tubular three dimensional surfaces, Nuovo Cimento, **11**(1989), 761-780.

[15] E. Kocakusaklı, O. O. Tuncer, I.Gök and Y. Yayli, A new representation of canal surfaces with split quaternions in Minkowski 3-space, Adv. Appl. Clifford Algebras 27 (2017) 1387ñ1409, doi:10.1007/s00006-016-0723-5.

[16] W. Lewis, Understanding novel structures through form-finding. Proceedings of the Institution of Civil Engineers, **158(4)**(2005), 178-185.

[17] Meinhardt Hans, The Algorithmic Beauty of Sea Shells, Springer, (2009).

[18] H. Moseley, On the Geometrical Forms of Turbinated and Discoid Shells, Phil. Trans. R. Soc. Lond. **128**(1838), 351-370.

[19] D. E. Moulton, A. Goriely, Surface growth kinematics via local curve evolution, J. Math. Bio. **68**(1-2)(2014), 81-108.

[20] D. M. Raup, A. Michelson, Theoretical Morphology of the Coiled Shell, Science, DOI: 10.1126/science.147.3663.1294, (1965).

[21] D. M. Raup, The Geometry of Coiling in Gastropods, Proc. Natl. Acad. Sci. U. S. A. **47**(4)(1961), 602-609.

[22] O. Roschel, Die Geometrie des Galileischen Raumes, Habilitationsschrift, Institut fur Math. und Angew. Geometrie, Leoben, (1984).

[23] Shoemake, K.: Animating rotation with quaternion curves. In: Proceedings of the 12th Annual Conference on Computer Graphics and Interactive Techniques (SIG-GRAPH '85), vol. 19, pp. 245–254, ACM, New York, NY, USA, 1985.

[24] G. Tuğ,Z. Özdemir, I. Gok, F. N. Ekmekci, Accretive Darboux Growth along a Space Curve, Appl. Math. Comp. **316**(2018) 516–524.

[25] G. Tuğ, Z. Özdemir, S. H. Aydin, F. N., Ekmekci, Accretive growth kinematics in Minkowski 3-space, Int. J. Geom. Methods Mod. Phys. **14**(2017), 1750069.

[26] I. M. Yaglom, A simple non-Euclidean Geometry and its Physical Basis, Springer-Verlag, New York, (1979).

[27] M. Zardini, Santiago Calatrava Secret Sketchbook. New York: Monacelli Press, (1996).

[28] Zöllner, A.M., Buganza, T.A., Gosain, A.K., Kuhl, E. Growing skin—tissue expansion in pediatric forehead reconstruction. Biomech. Mod. Mechanobiol., doi:10.1007/s10237-011-0357-4, in press.

[29] Zöllner, A.M., Buganza Tepole, A., Kuhl, E., 2012. On the biomechanics and mechanobiology of growing skin. J. Theor. Biol. 297, 166–175.